AI-AEC-13010

FORCED-FLOW SODIUM BOILING IN MULTIPLE CHANNELS

AEC Research and Development Report

Atomics International
North American Rockwell

P.O. Box 309
Canoga Park, California 91304

DISCLAIMER

LEGAL NOTICE

Printed in the United States of America
Available from
National Technical Information Service
U.S. Department of Commerce
Springfield, Virginia 22151
Price: Printed Copy $3.00; Microfiche $0.65

AI-AEC-13010
REACTOR TECHNOLOGY

FORCED-FLOW SODIUM BOILING IN MULTIPLE CHANNELS

By
D. LOGAN
C. J. BAROCZY
H. A. MOREWITZ

Atomics International
North American Rockwell

P.O. Box 309
Canoga Park, California 91304

CONTRACT: AT(04-3)-701
ISSUED: SEPTEMBER 15, 1971

DISTRIBUTION

This report has been distributed according to the category "Reactor Technology" as given in the Standard Distribution for Unclassified Scientific and Technical Reports, TID-4500.

ACKNOWLEDGMENT

The authors are grateful for the significant contributions made to this work by L. M. Haba, who performed loop operation and assembly, data acquisition, and assisted in data reduction; also to Dr. Louis Bernath, for many helpful discussions.

CONTENTS

TABLES

FIGURES

ABSTRACT

Experimental data are presented for the boiling sodium pressure drop - flow characteristic, at fixed power, for a group of interconnected channels formed by three heated 0.25-in. diameter pins located in a cloverleaf-shaped channel. Comparison of the data with a multichannel boiling sodium code shows reasonable agreement; however, the curve shape is shown to be very sensitive to small changes in flow-channel dimensions or geometry. Numerical results demonstrate that the pressure drop - flow behavior of a group of geometrically identical channels can, under nonuniform heat input conditions, be substantially different from that normally observed for a single channel. Boiling behavior and burnout heat flux data at 5 psia are also presented for a test section consisting of constant-geometry, equal-length, heated and unheated sections, with and without wire-wrap spacers. When the burnout heat flux data were corrected to constant pressure, velocity effects were negligible, while the effects of local subcooling were large.

THIS PAGE

WAS INTENTIONALLY

LEFT BLANK

I. INTRODUCTION

The occurrence of boiling in the sodium coolant of a Liquid Metal Fast Breeder Reactor (LMFBR) under accident conditions is, because of the interaction of coolant voiding and reactivity, an important consideration in the safety analysis of such reactors. Only by obtaining a reasonably good understanding of the boiling behavior of sodium in an LMFBR-like flow channel geometry can the necessary engineered safeguards be designed for the reactor. Because of the complexity of the sodium boiling process, attainment of the desired level of understanding requires both analytical and experimental work. It follows that the credibility of a particular analytical method is directly related to the degree to which the predictions are verified by meaningful experimental data.

The existence of a "check curve" in vertical, forced-flow boiling is well known, and is manifested as an increasing pressure drop characteristic with increasing flow in the all-liquid and high-mixture-quality region, and an increasing pressure drop with decreasing flow (Ledinegg instability) in the intermediate-mixture-quality region, all at the same input power. This leads to the condition of three flow rates being able to satisfy a given pressure drop, and, as such, provides the basis for possible flow excursions.

Studies conducted with SODIFAZE,[1] a steady-state, multichannel boiling sodium code, revealed that, under nonuniform heat input conditions, the pressure drop - flow characteristic (check curve) for three geometrically identical channels could be markedly different from that of a single channel. In contrast to a single channel, in which pressure drop increases rapidly when boiling starts, and continues to do so as flow decreases, the three-channel check curve can display a broad, virtually constant, pressure drop characteristic during the period when each of the channels successively attains boiling. Only when boiling is occurring in all channels does the three-channel check curve take on the steeply rising pressure drop profile which is typical of a single channel. Such a characteristic has significance to LMFBR's, as to the time available for corrective action when boiling occurs, and for indicating the lowered likelihood of boiling occurring simultaneously in a large fraction of a subassembly.

One objective of this work was to obtain experimental, boiling sodium check curves for a multichannel, LMFBR-like geometry, in order to verify the SODIFAZE code predictions. A favorable comparison is demonstrated between the experimental and numerical results. However, it is also shown that the check curve shape is very sensitive to small changes in flow-channel dimensions or geometry.

A second objective was to obtain data on the boiling behavior of sodium in an LMFBR-like multipin configuration, consisting of equal-length heated and unheated sections, with and without wire wrap. This investigation revealed the presence of a hysteresis effect, when decreasing flow was followed by increasing flow in the two-phase region.

A third objective was to obtain experimental data on burnout heat flux as a function of velocity and local subcooling. It is shown that when the data were corrected to constant pressure, the velocity effects were negligible, while the effects of local subcooling were large.

II. EXPERIMENTAL APPARATUS

A. TEST LOOP

A test loop is shown in a perspective drawing in Figure 1, and consists of an electromagnetic pump, flow control valve, economizer, preheater, test section with high-flux heater, condenser, and circulating cold trap. Virtually all of the loop is constructed of Type 304 stainless steel. Temperature, flow rate, pressure, and electrical power are measured and monitored at various locations. A detailed description of the loop is contained in Reference 2.

B. TEST SECTIONS

The three-pin test section is made in two parts, consisting of an insert which provides the desired sodium flow channel, and an external primary container (see Figure 2). The insert is fabricated from three 0.357-in. ID tubes (Type 304 stainless steel), which are milled to form a cloverleaf pattern which accommodates three 0.25-in. diameter pins with a triangular pitch-to-diameter ratio of 1.24 (the same as that in an FFTF fuel bundle). The three milled tubes are welded together, and then instrumented with numerous thermocouples and pressure tap holes which are aligned with holes in the primary container. A pressure tap tube is inserted through both holes to a flush position at the insert inside diameter, and then welded to the primary container. Shielded thermocouple tips probe through the insert wall; the wire runs between the insert and the primary container, and exits through a special adapter at the bottom of the primary container. The insert ends are fitted with a collar which prevents sodium flow from passing between the insert and the primary container.

The pressure drops across the 15 in. heated section, and the unheated 15 in. section (when used), were obtained by means of 0 to 300-in. water, Barton differential pressure transmitters. The static pressure at the end of the heated section was measured by a 0 to 50 psia Barton transmitter. Fluid temperatures in the various channels, when unwrapped heaters were used, were measured by immersion thermocouples, as shown in Figure 3a. When wrapped heaters were used, the thermocouples were placed inside the wire wrap, as shown in Figure 3b.

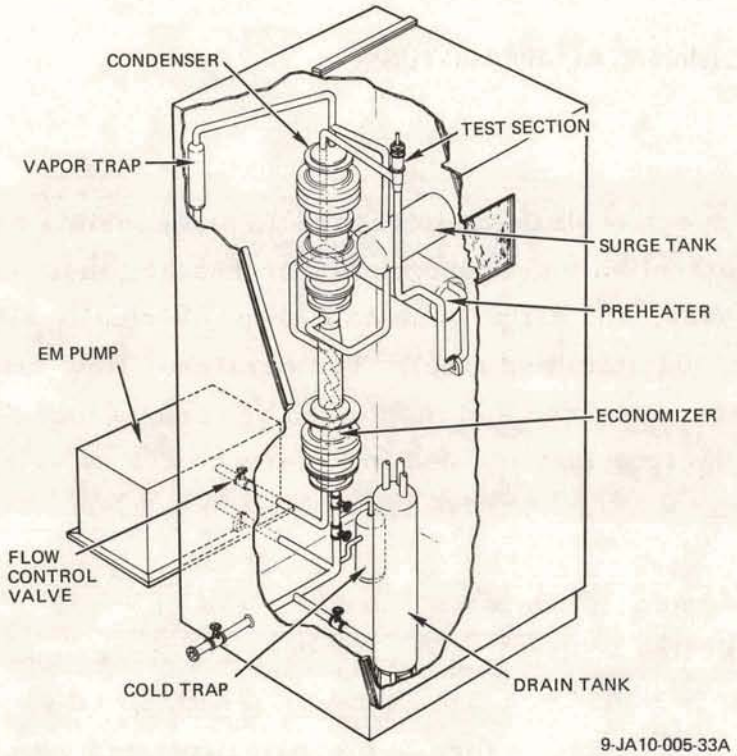

Figure 1. Two-Phase Sodium Loop

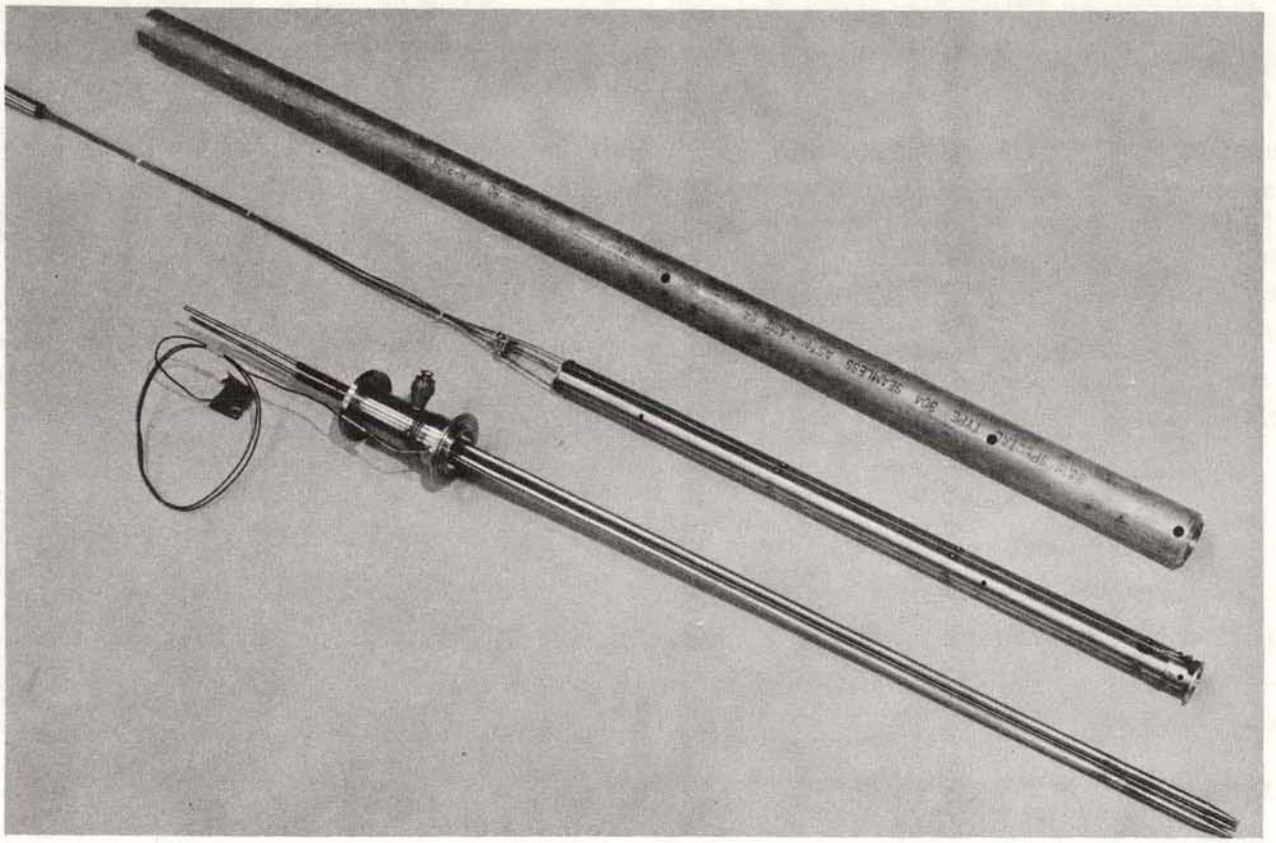

7702-40182

Figure 2. Heater Cluster and Test Section

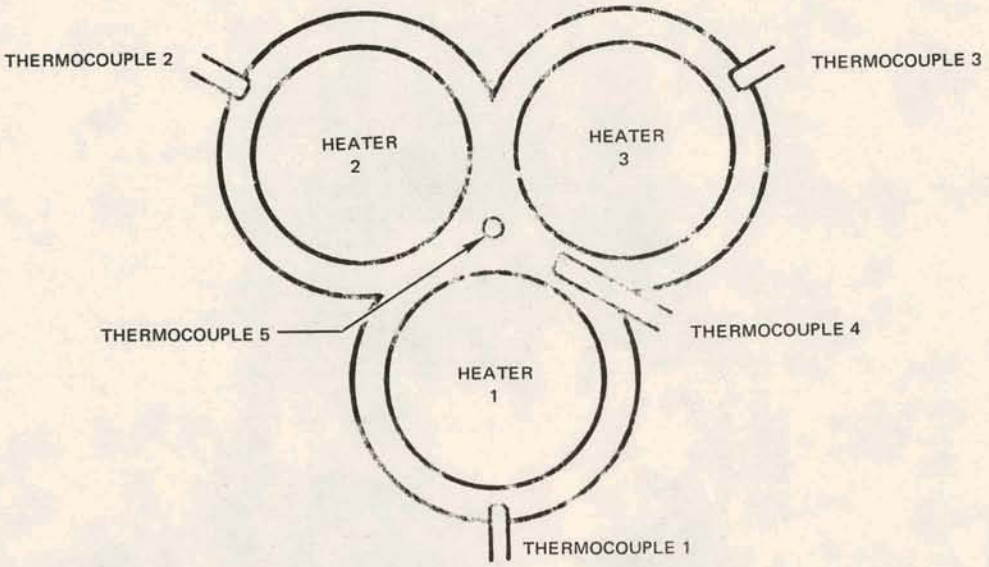

a. For Heaters Without Wire Wrap

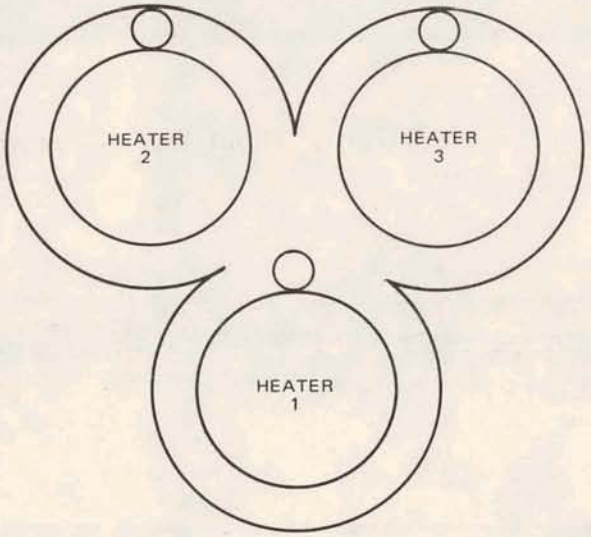

b. For Wire-Wrapped Heaters (Thermocouples located 3/4 in. downstream)

Figure 3. End-of-Heated-Zone Thermocouple Locations

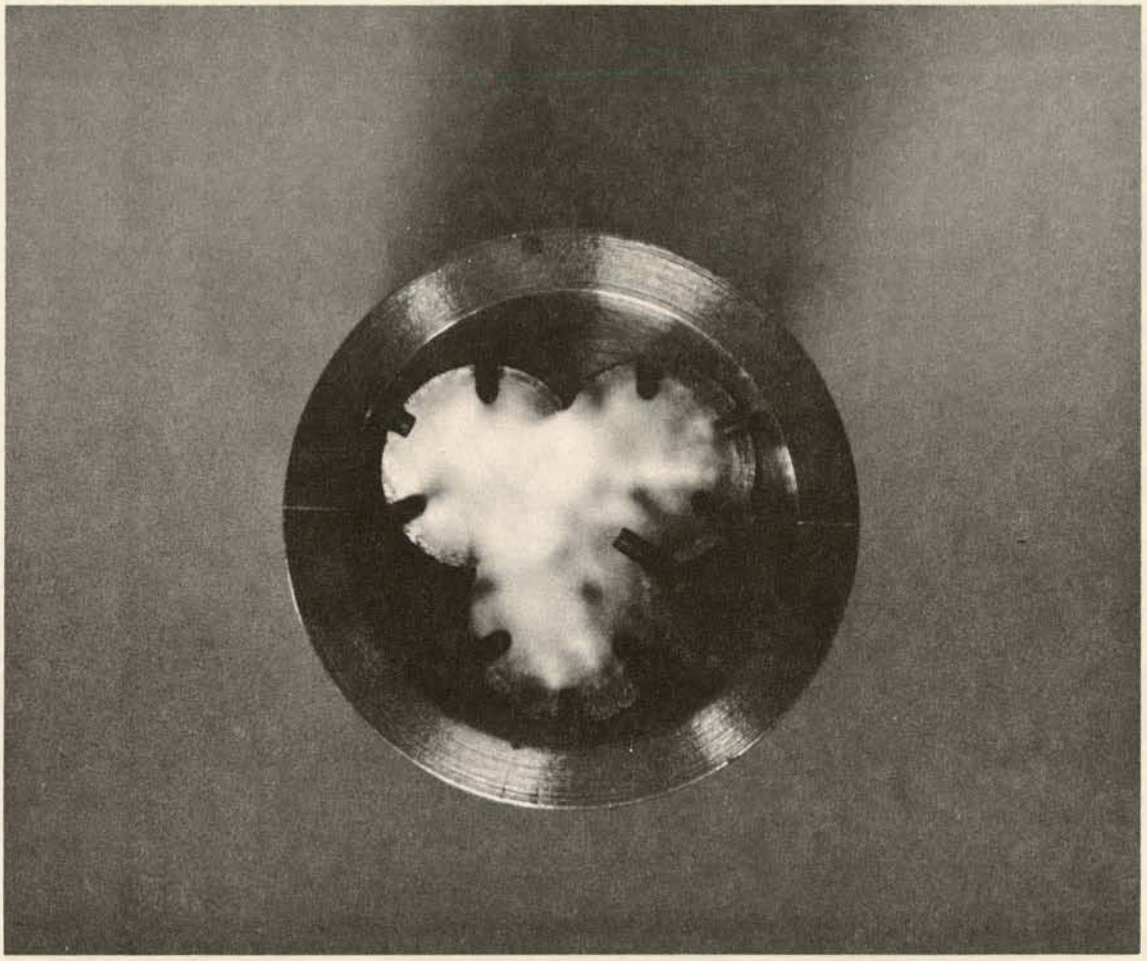

7702-40183

Figure 4. Test Section Without Wire-Wrapped Pins

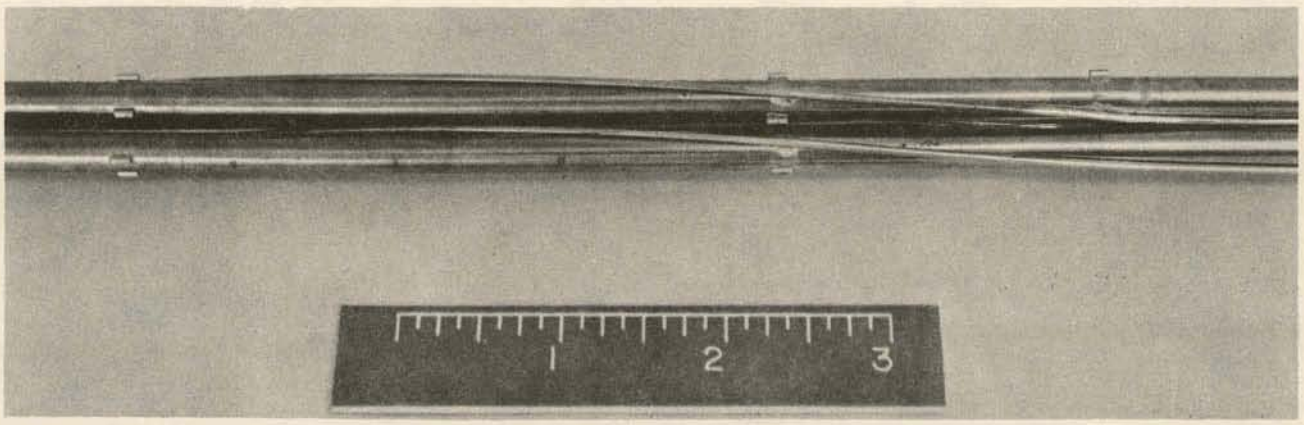

7702-40236

Figure 5. Wire-Wrapped Pins

The design concept of the three-pin test section was based on the attainment of equal fluid enthalpy increase in all channels when equal power was applied to each pin. This was accomplished by making the ratio of heated surface area to flow rate (for a given pressure drop) identical for all channels.

Two types of channel geometries, downstream of the heated pins section, were used in the boiling tests. In the first type, the exit flow from the three pins entered an expansion section which terminated in a 1-in. diameter pipe; tests conducted with this geometry are described in Section III-A. In the second type, the heated pin section was followed by an equal-length unheated section of identical geometry and size; tests conducted with this geometry (simulated LMFBR blanket region) are described in Section III-B.

C. HIGH-FLUX HEATER

The high-flux, electrically powered heater (shown in Figure 2) is a replaceable element that produces a uniform heat flux of known magnitude ($> 10^6$ Btu/hr-ft^2) at a sodium temperature of 1600°F. The main components of the heater consist of a body assembly, tantalum sheath, graphite heating element, boron nitride sleeve, and electrode.

The boron nitride sleeve is slip fitted into the sheath, and insulates all but the grounded end of the graphite heating element from the sheath. A spring-loaded electrode, which is maintained in alignment by insulated bushings, permits an input of up to 24 kw of ac power to a 15-in. long heater. The three heaters were "Y" connected, so that the grounded ends were electrically neutral. The sodium at the grounded end of the electrode provides a short current return path to the outer wall of the test section.

Positioning of the three heaters within the flow channel was provided by pins located every 5 in. along the heated length, and by two internal spacers located at the 1/3 and 2/3 points in the heated length (see Figure 4), or by 52-mil diameter wire wrap on a 12 in. pitch with extra spacers every 4 in. to simulate adjacent wire-wrapped pins (see Figure 5).

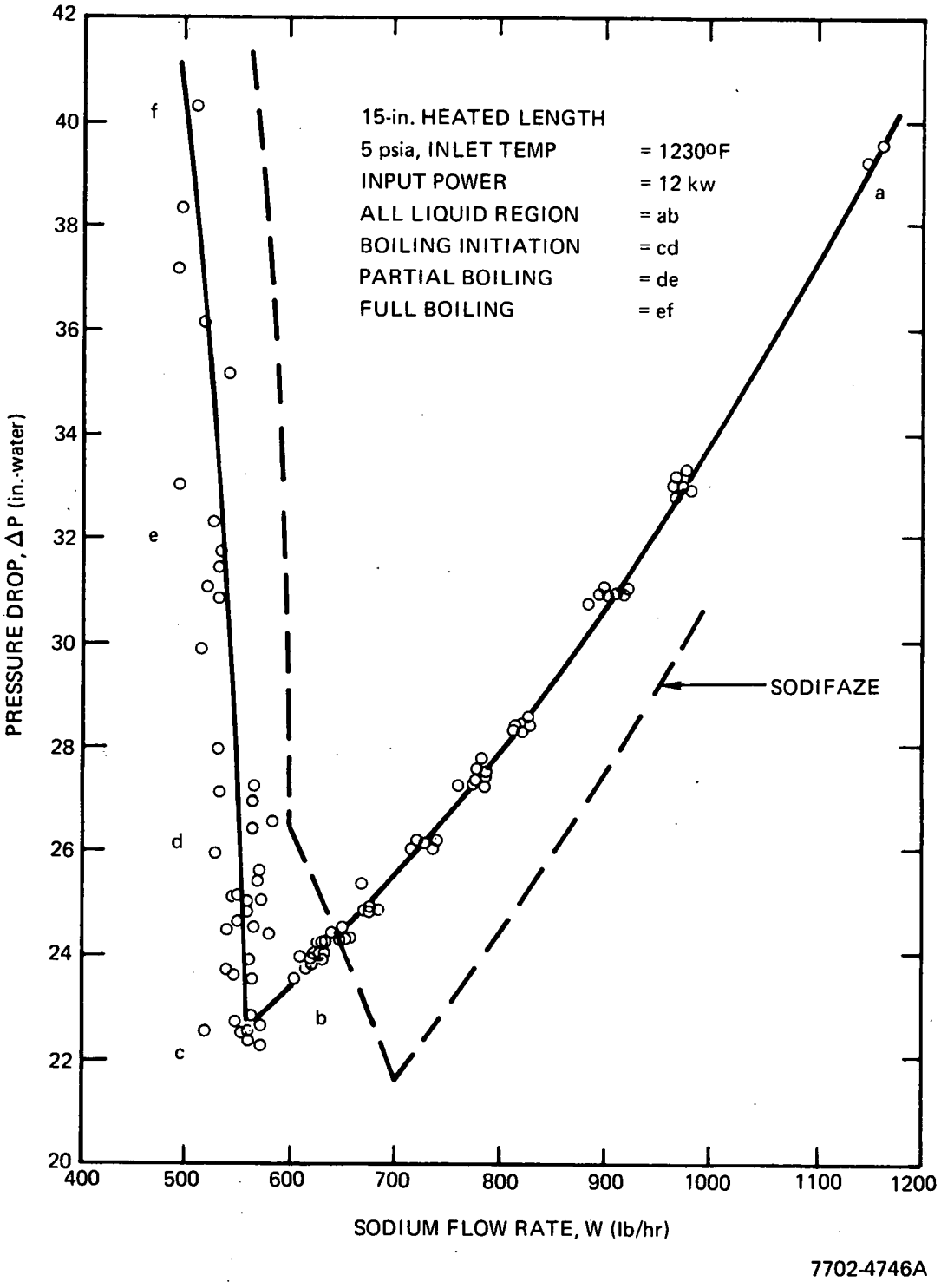

Figure 6. Check Curve for 3-Channel Test Section, Test 1

III. CONTINUOUS BOILING

Using the three-pin cluster and test section described previously, continuous boiling sodium tests were performed to obtain the pressure drop - flow characteristics of this multichannel configuration. Typically, pressure, inlet temperature, and heat input were fixed, and sodium flow rate was then increased (or decreased) over a wide range. Steady-state conditions were maintained for at least 30 sec at each flow rate. The EM pump was isolated from flow fluctuations in the test section by a control valve (Δp = 60 psi) at the pump exit. Thermocouple and flow channel locations and designations are shown in Figure 3.

A. TEST SECTION WITH LARGE-AREA EXIT SECTION

1. Experimental Data

Figure 6 shows the check curve obtained by holding total heater power constant, at ~12 kw, and gradually increasing sodium flow rate (1000 lb/hr corresponds to 5.9 ft/sec average liquid velocity). During the run, the power to each heater was held constant, but not equal, as the highest power heater (No. 3) had ~15% greater power input than the lowest power heater (No. 1).

The check-curve characteristic shown in Figure 6 is as expected: in the all-liquid region, pressure drop decreases as flow decreases; in the boiling region, pressure drop increases as flow decreases. Using the actual heat input and the design geometry (Figure 3), the SODIFAZE code prediction[1] is seen to compare favorably* with the experimental check curve. Furthermore, as identified by letters on the check curve, distinctive regions are evident, based on the measured fluid temperatures in the various channels shown in Table 1. In the all-liquid region (ab), the fluid temperatures in the channels are close to, or below, saturation. In the boiling initiation region (cd), the channel temperatures range from below saturation (No. 1) to 66°F liquid superheat (No. 3, 4). In the partial boiling region (de), the channel temperatures may be below (No. 1), above (No. 2, 3), or at (No. 4, 5) saturation; at the latter locations, boiling is presumed

*Considering the uncertainties in the input data to SODIFAZE (smooth tube friction factor, two-phase pressure drop - void fraction correlations), the observed differences are relatively modest.

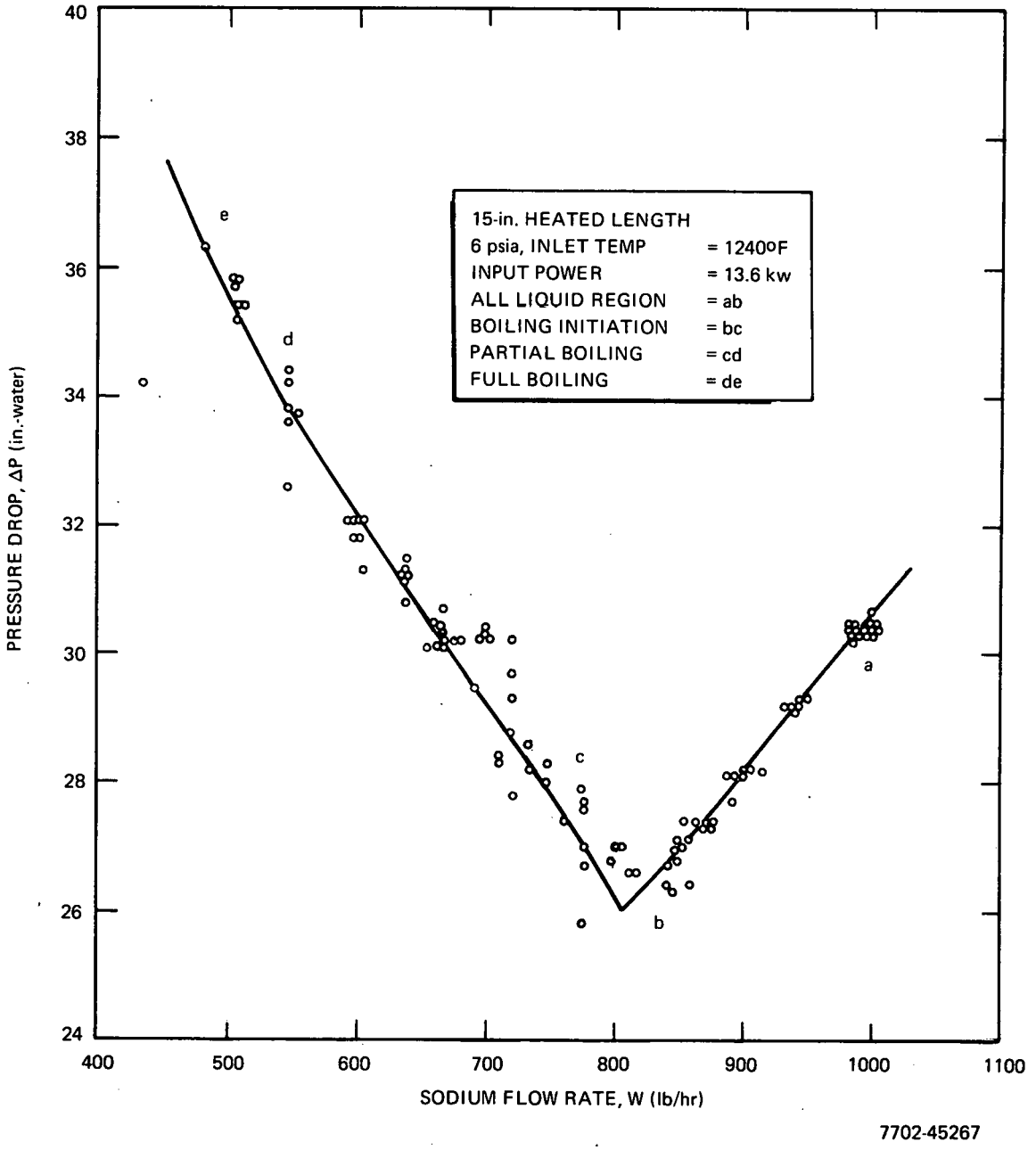

Figure 7. Check Curve for 3-Channel Test Section, Test 2

TABLE 1

FLUID TEMPERATURES
(Test 1)

Region	Thermocouple Location					
	1	2	3	4	5	T_{sat}
	Temperature (°F)					
ab (All-Liquid)	1318	1353	1422	1403	1408	1412
cd (Boiling Initiation)	1379	1446	1501	1499	1448	1435
de (Partial Boiling)	1399	1447	1444	1426*	1433*	1431
ef (Full Boiling)	1421*	1413*	1413*	1410*	1410*	1414

*Boiling

to be occurring. In the full boiling region (ef), the fluid temperatures are essentially equal to one another, and to saturation temperature, as determined from the measured static pressure.

Although further confirmation is required, the present data (partial boiling region) indicate that it is possible for subcooled liquid, superheated liquid, and boiling liquid to coexist in a geometry consisting of LMFBR-like interconnected channels. However, this apparent lack of communication between channels would be expected to be greatly diminished, if wire wrap spacers were used (see Section III-B).

Figure 7 shows the second check curve (Test 2), which was obtained by decreasing flow rate, rather than by increasing flow rate (as was done with the first and third check curves), at fixed power. In contrast to the steep boiling pressure drop - flow characteristic of the first check curve, this one exhibits a rather flat profile. It appears possible that, as total flow rate is increased, the channel with the greatest mixture quality may, through a delay in flow distribution, cease boiling at a greater total flow rate than that at which boiling commenced (in the same channel) with decreasing flow rate (see Section III-B).

The various regions, and the attendant fluid temperatures for the check curve in Figure 7, are shown in Table 2.

TABLE 2
FLUID TEMPERATURES
(Test 2)

Region	Thermocouple Location					
	1	2	3	4	5	T_{sat}
	Temperature (°F)					
ab (All-Liquid)	1336	1380	1401	1432	1432	1440
b (Boiling Initiation)	1340	1386	1405	1455	1443	1440
c (Partial Boiling)	1351	1416	1432	1432	1439*	1440
cd (Partial Boiling)	1425	1446*	1449*	1447*	1448*	1450
de (Full Boiling)	1471*	1465*	1465*	1463*	1468*	1468

*Boiling

Some of the flat pressure drop characteristics are attributable to the increasing pressure level as flow decreases; this, in effect, reduces the mixture quality (and pressure drop) which would otherwise result. Simultaneous "burnout" of two of the three heaters occurred immediately after taking the data at Location e. At burnout, the following conditions prevailed: (1) maximum heat flux, 253,000 Btu/hr-ft^2, (2) average mass velocity, 502,000 lb/hr-ft^2, (3) average mixture quality, 0.011, and (4) saturation temperature, 1479°F. By use of the observed maximum heat flux, and by estimating the wall minus bulk temperature to be that of the melting point of tantalum minus the sodium saturation temperature, a heat transfer coefficient of ~64 Btu/hr-ft^2-°F is obtained. Such a low heat transfer coefficient is representative of the film boiling region. Additional burnout data are contained in Section III-C.

Figure 8 shows the third experimental check curve (Test 3), which displays a pronounced looping characteristic, similar to that predicted by SODIFAZE for nonuniform flow geometry or heat input conditions. The experimental curve shows pressure drop to decrease with decreasing flow in the all-liquid region (ab). At boiling initiation (bc), with attendant liquid superheat (Table 3), pressure drop increases very rapidly, to a moderate extent. In the partial boiling regions (cd, de), pressure drop decreases with decreasing flow to the level existing at boiling initiation, and then begins to increase. In the full boiling region (ef), with boiling in all channels, pressure drop starts to increase rapidly. The fluid temperatures and saturation temperatures in the various channels, and the boiling regions inferred from them, are shown in Table 3.

2. Comparison of Experimental Data with SODIFAZE Code

Detailed comparisons between the experimentally obtained 3-pin looping check curve (Figure 8) and SODIFAZE predictions were made. Figure 9 shows the flow channel arrangement, consisting of seven channels of three types. By combining the three-channel 4's into a single channel, a five-channel configuration was obtained, and used for code purposes.

Previously, it was observed that the actual all-liquid temperature rises in Channels 1 and 2 were less than, and in Channels 4 and 5 greater than, those calculated by the code for the experimental heat inputs and design geometry. For a given pressure drop and fluid properties, the liquid flow rate in a channel varies as the product of channel flow area (A) and the two-thirds power of the hydraulic diameter (D). Since the actual liquid temperature increase varies inversely with actual flow rate, it is possible to solve for the existing channel flow areas and hydraulic diameters. As this solution procedure becomes tedious when the pins are shifted, Heaters 1 and 2 were, instead, each moved 0.010 in. toward the center, on a 30° angle from the horizontal. This produced a change in both the channel flow areas and the channel heat inputs. This condition is called the "altered geometry," whereas the original heater placement is called the "design geometry." A condition intermediate to the two named above is referred to as the "intermediate geometry." The results of SODIFAZE code runs made with each of the above conditions are described in the following paragraphs.

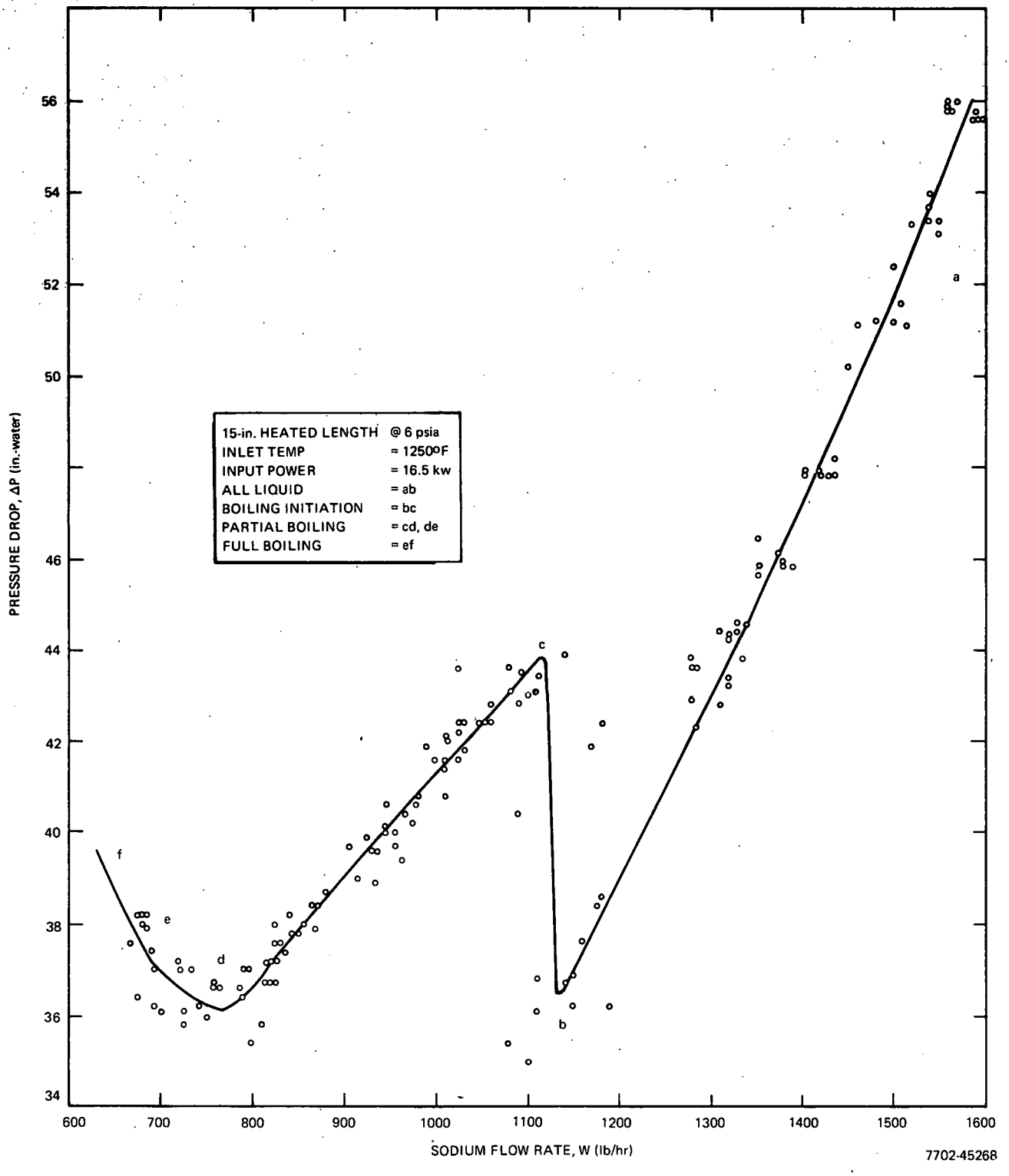

Figure 8. Check Curve for 3-Channel Test Section, Test 3

TABLE 3

FLUID TEMPERATURES

(Test 3)

Region	Thermocouple Location					
	1	2	3	4	5	T_{sat}
	Temperature (°F)					
ab (All-Liquid)	1327	1349	1406	1431	1445	1460
b (Boiling Initiation)	1359	1386	1452	1498	1492	1464
c (Partial Boiling)	1345	1389	1444	1448	1461*	1463
cd (Partial Boiling)	1371	1436	1461*	1461*	1462*	1464
de (Partial Boiling)	1435	1464*	1470*	1468*	1468*	1467
ef (Full Boiling)	1460*	1460*	1461*	1458*	1462*	1461

*Boiling

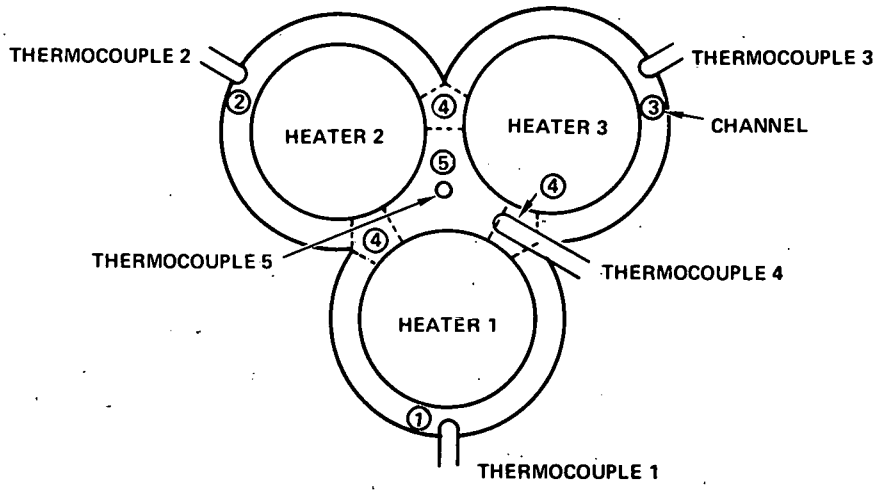

Figure 9. Flow-Channel Cross Section

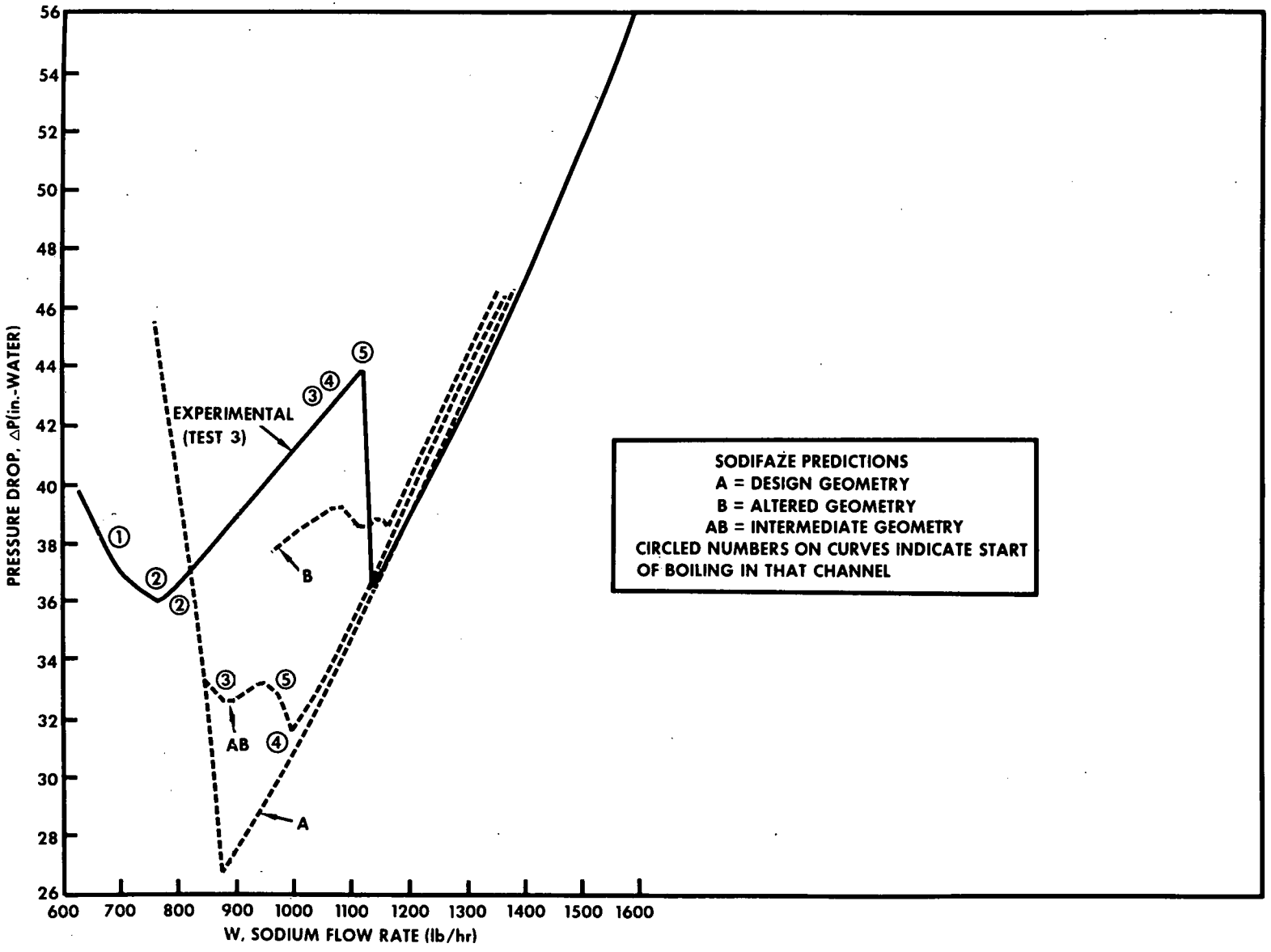

Figure 10. Comparison of Experimental and Predicted Check Curves

Figure 10 shows the experimental looping check curve (from Figure 8), in comparison with the code predictions. In order to match the predicted all-liquid pressure drop with that observed, it was necessary to increase the all-liquid, smooth-tube, friction factor in the code by 30%. The observed higher pressure drop is thought to be the result of the relatively rough, pitted surface of the "as-received" tantalum tubing used in these tests.

Using the design geometry, the predicted check curve (A) is shown to start boiling at a lower flow rate than observed, and to be without loops. This is the check curve shape to be expected for a single channel, or a group of channels with identical fluid enthalpies at any point in the heated length. Indeed, the shape of the check curve is determined by the boiling sequence of each channel, which, in turn, is determined by the order in which the liquid in each of the channels reaches saturation conditions. If, as in this case, boiling is attained in all channels over a very limited flow-rate range, no loops can occur. Naturally, it follows that the order in which the fluid in each channel reaches saturation (or superheat) conditions in the experiment must be matched by the code, if the resulting check curve shape is to be duplicated.

The predicted check curve (B) for the "altered geometry" is shown to start boiling at about the same flow rate as observed experimentally, and also to have a shape similar to that of the experimental check curve. However, the predicted check curve shows that only Channels 4 and 5 are boiling when the curve ends, because the criterion that equal pressure drop exists across every channel node can no longer be fulfilled. That is, as total flow is decreased and the fraction of total flow in the boiling channels is reduced, relative to the nonboiling channels, a point is reached where the required liquid flow diversion (as prescribed by equal pressure drop) from the boiling channels to the nonboiling channels is greater than the flow in the boiling channels.

The predicted check curve corresponding to a condition intermediate (with respect to channel flow areas and heat inputs) to the two described previously is shown as AB in Figure 10. Although the predicted curve shows boiling to start at a lower flow rate than observed, and to cover a narrower flow-rate range, the correspondence between predicted and observed check curve shapes is very good. Furthermore, as shown by the circled numbers on the curves,

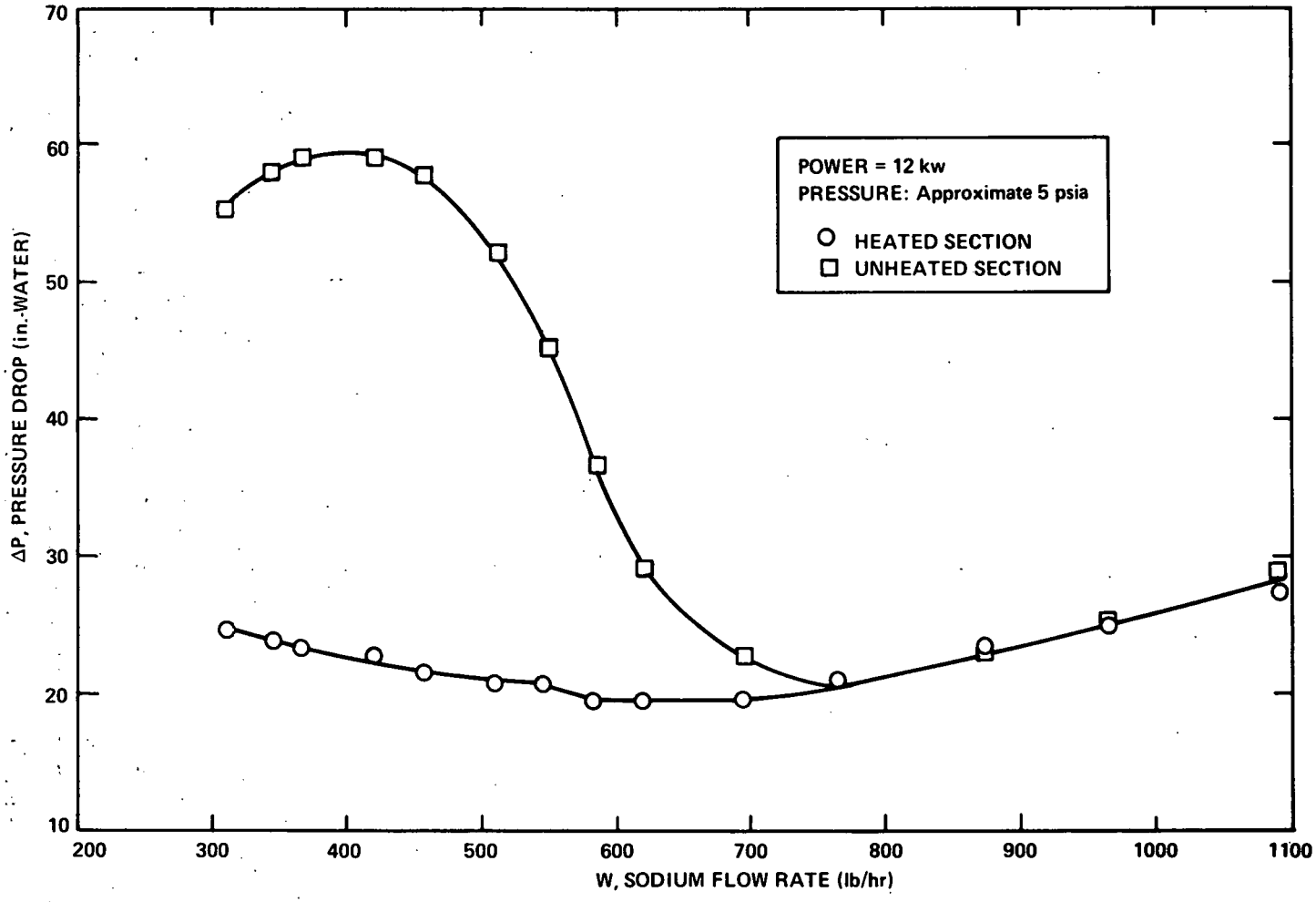

71-A1-23-3

Figure 11. Pressure Drop vs Flow Rate for Heated and Unheated Test Sections (Power = 12 kw)

the sequence of boiling among channels is fairly well matched between the predicted and observed check curves.

These results indicate that the actual geometry of the test section corresponds most nearly to that of the assumed intermediate geometry. However, it is evident that, for test sections such as used here (3 closely spaced, 0.25-in. diameter pins with intermittent spacers), the shape of the check curve can be substantially affected by very small changes in individual channel dimensions or geometries. (Presumably, the use of wire wrap on pins, as in the LMFBR core, would ameliorate this condition somewhat. Typically, LMFBR designs have ±0.005 in. tolerance between pins with wire-wrap spacers.)

B. TEST SECTION WITH EQUAL HEATED AND UNHEATED LENGTHS

As a further step toward more closely simulating LMFBR core geometry with the present 3-pin test section, an unheated 3-pin, 15-in. long section was added downstream of the heated 3-pin, 15-in. long section. For each section, the geometry and flow area are identical. As such, this test section more nearly duplicates the LMFBR core, by providing, on a reduced-length basis, the appropriate hydraulic equivalent of the reactor blanket area.

1. Pins Without Wire Wrap

The behavior of this configuration was explored by running three check curves (pressure drop vs flow rate) with boiling sodium, each with a different heater input. In each case, boiling was observed in the heated section; and, in the two highest-power tests, flashing apparently occurred in the unheated section when superheated ($\Delta T > 30°F$) liquid sodium exited from the heated section. Figure 11 shows the first check curve obtained with a total power input of 12 kw. As the all-liquid region ends, at ~760 lb/hr, the pressure drop in the heated section becomes constant as the pressure drop in the unheated section increases rapidly. As flow is further decreased, the pressure drop in both sections increases, reaches a peak in the unheated section, and then starts to decrease. For the same flow rate, in the boiling region, the much larger pressure drop in the unheated section, compared with the heated section, is due to the presence of two-phase flow along the entire length of the unheated section, and only part of the length in the heated section.

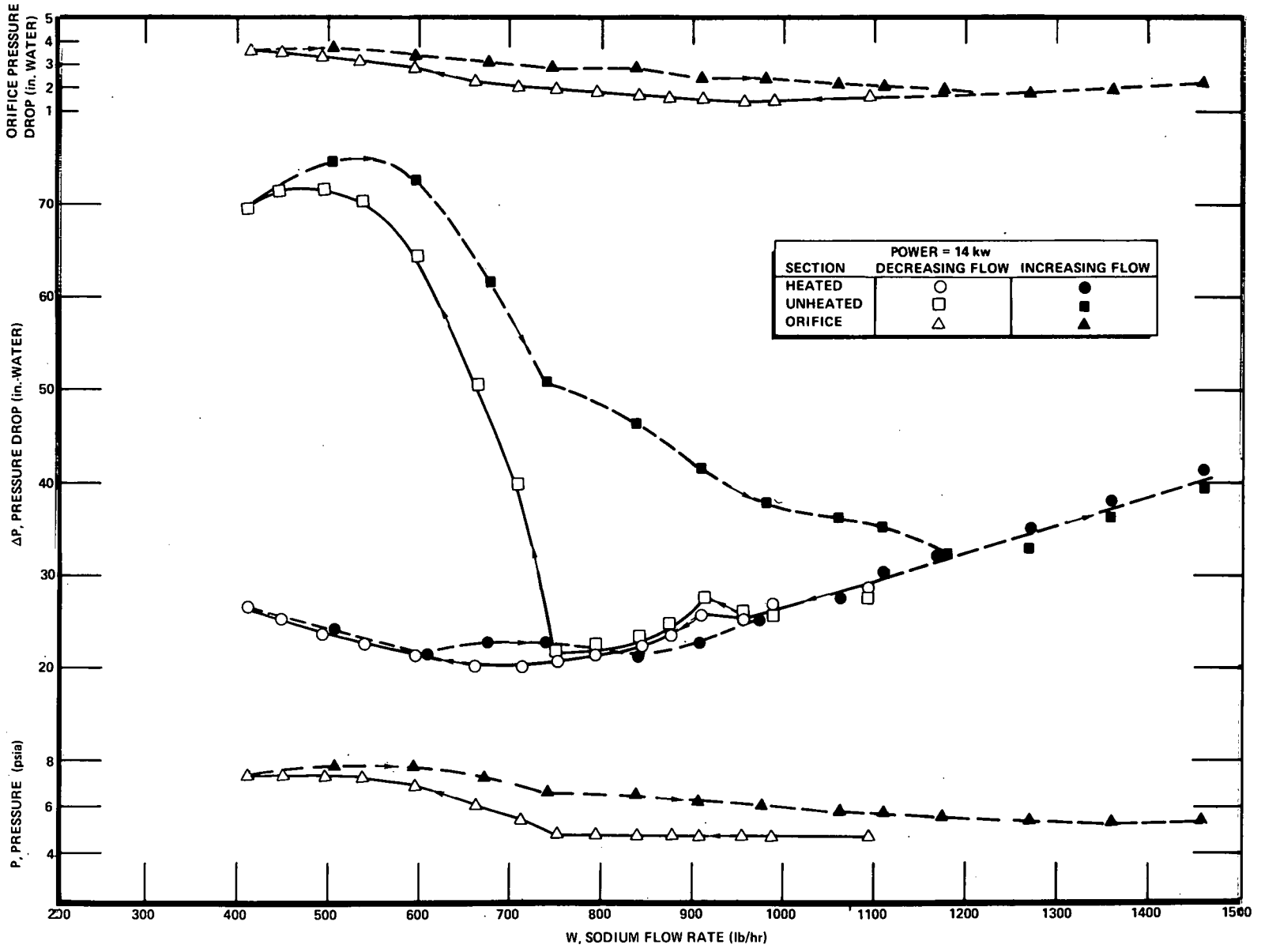

71-A1-23-4

Figure 12. Pressure and Pressure Drop vs Flow Rate for 3-Pin, Heated and Unheated Test Sections (Power = 14 kw)

The second check curve, taken with 14-kw power input, is shown in Figure 12. In addition to the section pressure drops, the static pressure at the end of the heated section and the orifice pressure drop are shown, both for decreasing and increasing flow. With decreasing flow, it is seen that, at ~960 lb/hr, premature boiling starts, and then ceases. Sustained boiling, with attendant increasing pressure drop in both sections, begins at 750 lb/hr. Coincidentally, the static pressure at the end of the heated section, and the orifice pressure drop, also start to increase at this point. In the boiling region, with decreasing flow, pressure drop increases for both sections, reaching a peak in the unheated section.

With fixed power, increasing flow rate shows the unheated section to exhibit a distinct hysteresis effect which coincides with the decreasing pressure level. As a result, two-phase flow in the unheated section ceases at a considerably greater flow rate than that at which it began. The behavior patterns of the static pressure and orifice pressure drop are very similar to those of the unheated section.

The third check curve, for 16-kw power input, is shown in Figure 13. The general pattern of behavior is similar to that described in Figure 12, with the following exceptions.

The unheated section pressure drop increase, at premature boiling (980 lb/hr), is much greater than that observed for 14 kw, while the heated section pressure drop is much less, being essentially that of all-liquid flow. This effect appears to be the result of superheated ($\Delta T \sim 60°F$) liquid leaving the test section, and subsequent flashing of the liquid in the unheated section.

Unlike the steadily increasing boiling pressure drop shown in Figure 12 for the heated section, the check curve in Figure 13 displays pronounced loops, with the same shape as previously shown (Figure 8) for the 3-pin test section without an unheated section, for the same power input (16 kw). The lower pressure drop for the check curve in Figure 13, compared to Figure 8, is believed to be the result of the smooth-surface tantalum tubing used for the heater cladding in the Figure 13 test. Confirming this observation is the fact that the all-liquid friction pressure drop (excluding static head, which appears in the figure) for the

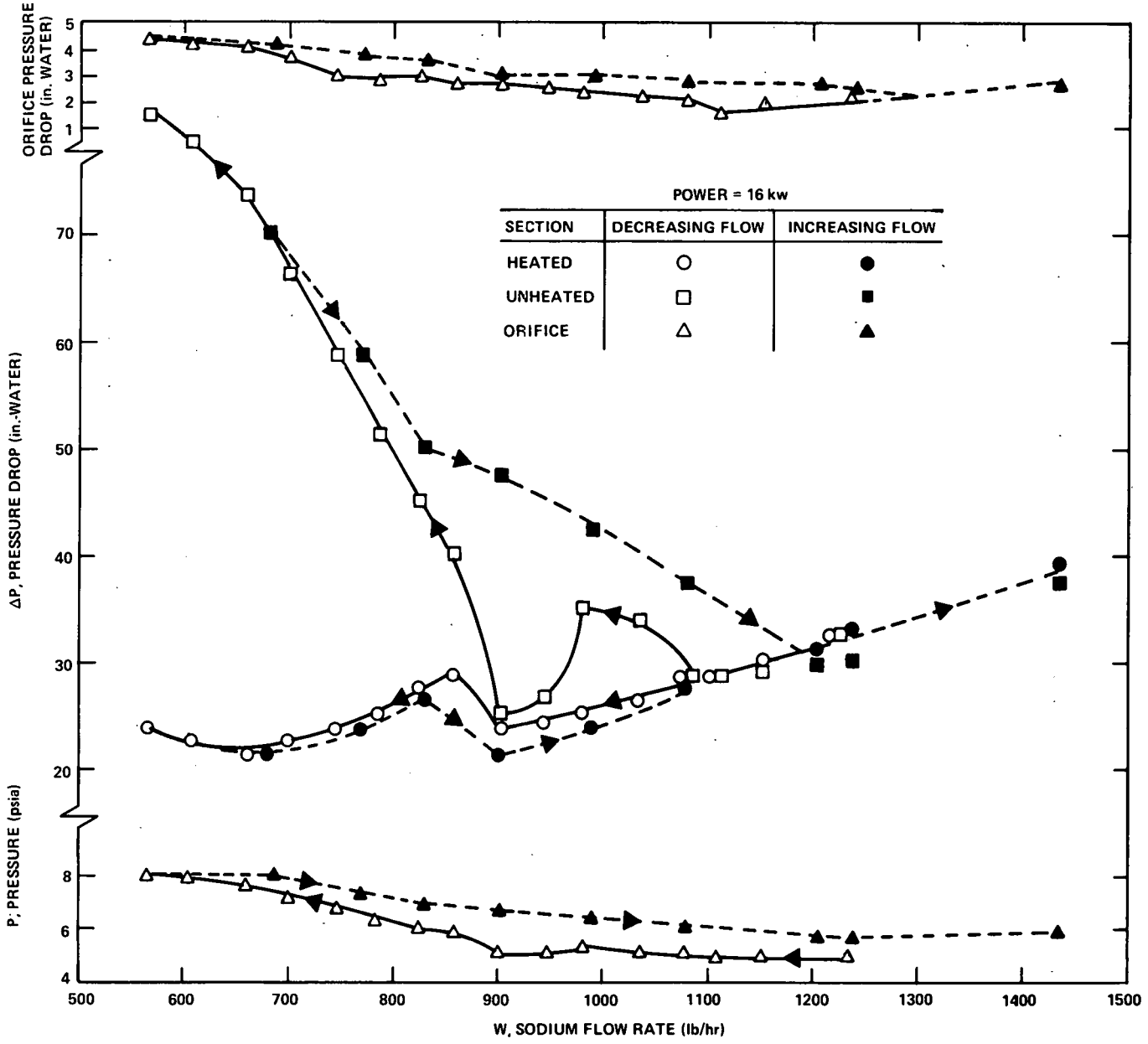

Figure 13. Pressure and Pressure Drop vs Flow Rate for 3-Pin, Heated and Unheated Test Sections (Power = 16 kw)

71-A1-23-5

Figure 13 test section is ~25% less than that for the Figure 8 test section. Since the two-phase pressure drops are primarily multiples of the all-liquid pressure drop, the observed differences in pressure drop, between Figure 13 and Figure 8, are as expected.

2. Pins with Wire Wrap

As a continuation of the process of achieving a more complete representation of an LMFBR core, wire-wrap spacers were added to the 15 in. heated and 15 in. unheated test sections. Boiling tests, utilizing three heated pins, were conducted at total power inputs of 16, 25, and 32.4 kw; additional tests, to burnout, were performed with two heated pins, and then with one heated pin.

Figure 14 shows representative traces for the 16-kw boiling run in which flow was decreased and then increased. Shown are static pressure, pressure drops across the heated and unheated sections, flow rate, and accelerometer output. As flow decreases in the all-liquid region, the heated and unheated section pressure drops decrease, as the static pressure remains constant.

A flattening of the pressure drop (indicating two-phase flow) occurs first in the unheated section, and then in the heated section. As flow is further reduced, both the static pressure and the unheated section pressure drop increase substantially, while the heated section pressure drop remains essentially constant. As flow is then increased, the process is reversed, except for some hysteresis effect in the pressure drops and static pressure; that is, higher levels exist on the increasing flow portion of the process. The unheated section pressure drop shows oscillations, and a pressure increase above the liquid base, in the same interval that large oscillation amplitudes occur on the accelerometer trace.

Figure 15 shows bulk fluid temperature traces for the end of the heated section (upper trace) and the end of the unheated section (lower trace) for the same 16-kw run. It can be seen that the rising and falling pattern of the static pressure at the end of the heated section is duplicated by the temperature trace at the end of the heated section. In contrast, the temperature trace at the end of the unheated section is much flatter. For saturation conditions at both the end of the heated section and unheated section, the previously described pattern is as expected, if the downstream pressure remains essentially constant.

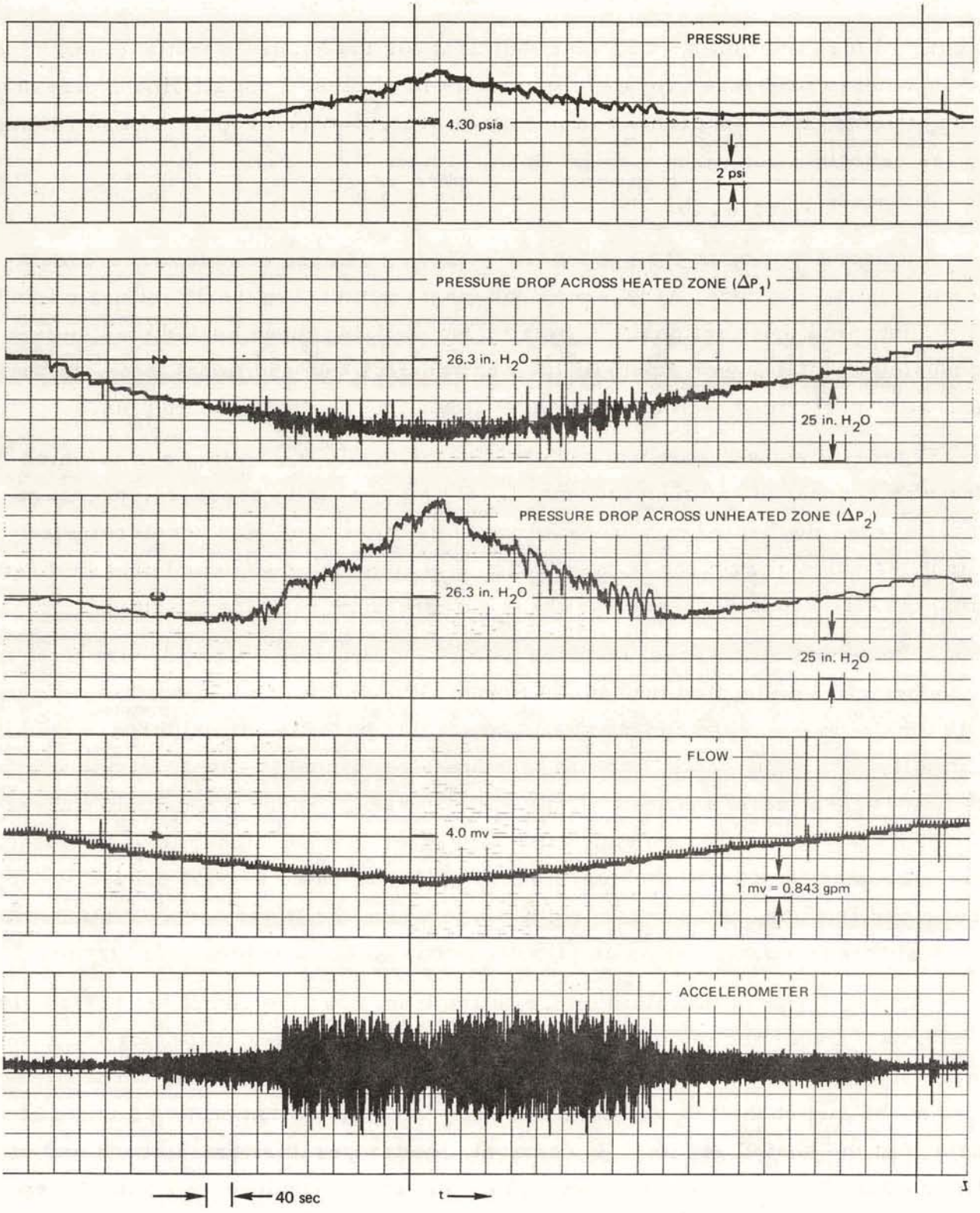

Figure 14. Traces for 16-kw Total Power Boiling Run
(3 wire-wrapped pins, 15 in. heated and
15 in. unheated test sections)

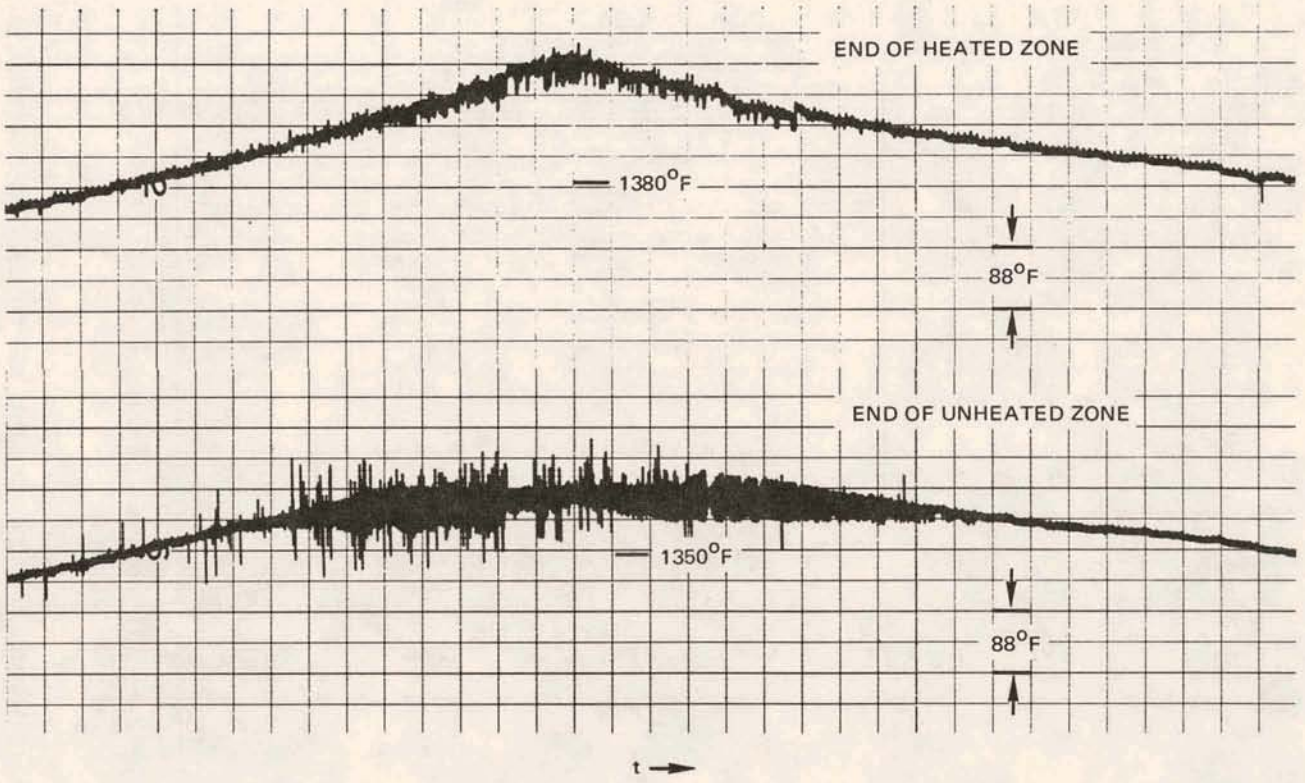

Figure 15. Bulk Fluid Temperature Traces for 16-kw Total Power Boiling Run (3 wire-wrapped pins, 15 in. heated and 15 in. unheated sections)

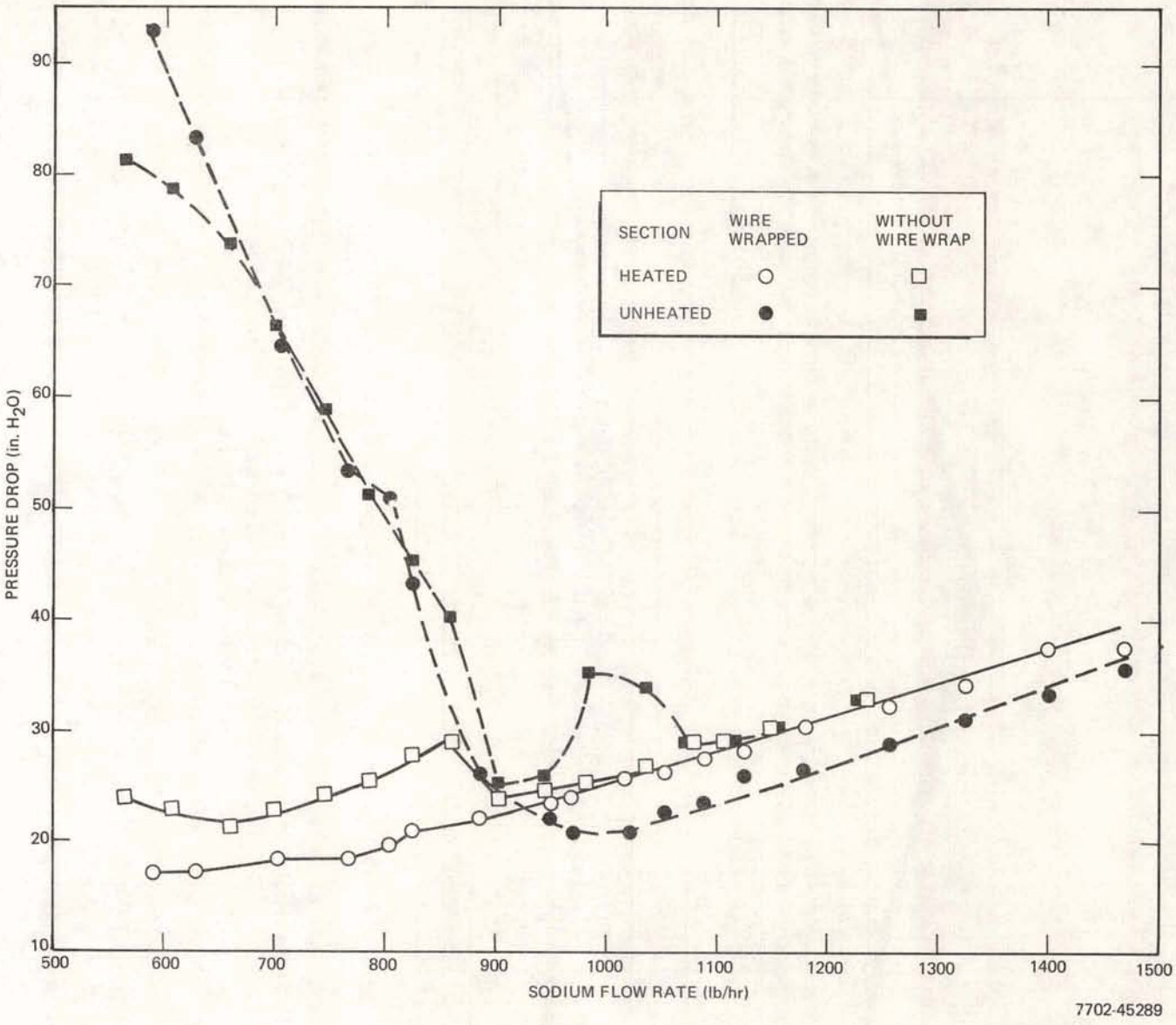

Figure 16. Comparison of Check Curves Obtained With and Without Wire Wrap [3-pin, 15 in. heated and 15 in. unheated sections, 16-kw heat input (4.25 kw/ft)]

3. Boiling Behavior, With and Without Wire Wrap

In the cases of two sets of boiling tests, at 16 kw and ~33 kw, conditions were generally similar, except for the use of wire-wrap spacers in the second set of tests. Thus, these tests afford a means for evaluating possible differences in boiling behavior between the two types of flow configurations.

Figure 16 shows pressure drop as a function of sodium flow rate, with a total heat input of 16 kw. This corresponds to average (per pin) conditions of 4.25 kw/ft and a heat flux of 222,000 Btu/hr-ft^2. In the all-liquid region (decreasing pressure drop with decreasing flow rate) the heated and unheated section pressure drops for the unwrapped configuration are identical. For the wire-wrap case, the unheated section pressure drop is slightly lower than that of the heated section. Overall, the pressure drops for both the wire-wrapped and unwrapped configurations are essentially equal.

As a result of unequal enthalpies in the various channels, in the unwrapped case, superheated liquid leaving the heated section flashes in the unheated section, creating a temporary increase in the unheated section pressure drop. In contrast, the wire-wrap configuration does not exhibit such behavior, but instead, shows a smooth transition between all-liquid and two-phase flow conditions in the unheated section.

Boiling in the heated section of the unwrapped configuration is manifested as a looping check curve; whereas, for the wire-wrap case, the pressure drop exhibits a modest increase over that for all-liquid flow. In both cases, however, the unheated section pressure drops are nearly identical.

Figure 17 shows total pressure drop as a function of flow rate for 34.6 kw (9.2 kw/ft, 480,000 Btu/hr-ft^2) with unwrapped pins and 32 kw (8.5 kw/ft, 444,000 Btu/hr-ft^2) for the wire-wrap pins. In the all-liquid region, the heated and unheated section pressure drops for the wire-wrap configuration are a little greater than those for the unwrapped configuration.

For the wire-wrap section, boiling in the heated section is indicated by a modestly increasing pressure drop with decreasing flow until burnout is reached. Concurrently, the pressure drop in the unheated section shows a slight flattening, but a predominately liquid characteristic (decreasing pressure drop with decreasing flow). For the unwrapped pins, boiling in the heated section is indicated

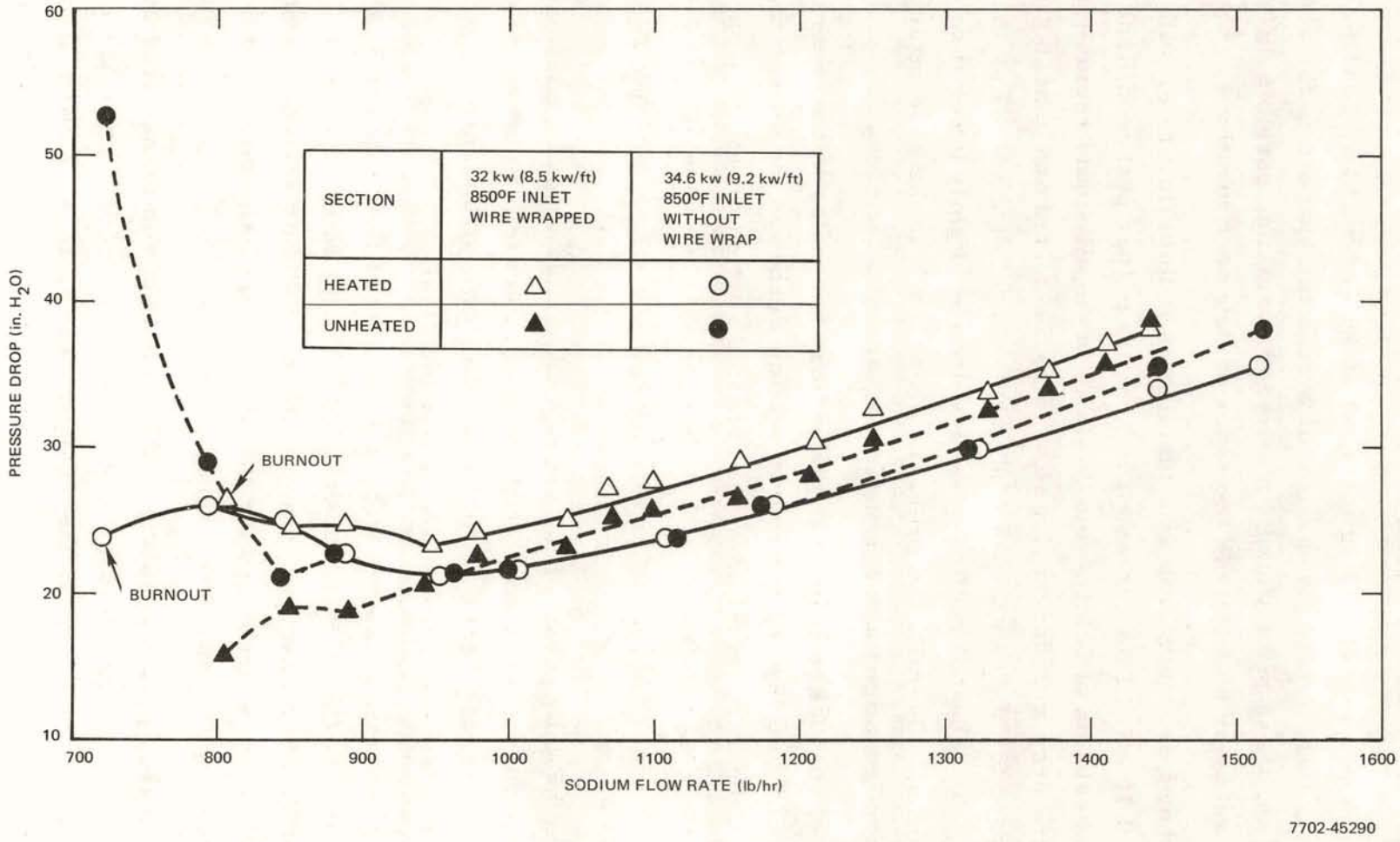

Figure 17. Comparison of 3-Pin Wire-Wrapped and Unwrapped Boiling Tests (15 in. heated and 15 in. unheated test sections)

by a very gradually increasing pressure drop, which reaches a peak and then decreases as burnout is reached. At the same time, the pressure drop in the unheated section increases, decreases, and then rapidly increases, reaching a magnitude that is more than twice that in the heated section. The much higher pressure drop in the unheated section of the unwrapped pin configuration (compared to the wire-wrap case) is the result of the greater mixture quality which accompanies the lower flow rate at burnout.

The smoothness of the pressure drop - flow characteristic of the wire-wrap heated section (no loops), compared to the unwrapped heated section, and the absence of flashing due to superheated liquid sodium, may be due, in part, to the improved interchannel mixing afforded by the wire wrap. However, examination of the data shows that the wire-wrap configurations have a nearly uniform power distribution, among pins, whereas the unwrapped configurations have a decidedly nonuniform distribution. For example, the following maximum power ratios, among pins, exist: wire wrap, 1.09 (16 kw), 1.06 (32 kw); unwrapped, 1.11 (16 kw), 1.32 (34.6 kw). These conditions, in turn, are reflected as close to uniform liquid enthalphy (via outlet temperature) for the individual channels in the wire-wrap case, and substantial differences among individual channel enthalpies for the unwrapped case. Thus, in the wire-wrap case, the transition to boiling is very smooth and uniform.

C. BOILING BURNOUT INVESTIGATIONS

During the course of the 3-pin boiling experiments, burnout conditions were achieved on seven occasions. As used here, burnout corresponds to the occurrence of either melting of the heater cladding, as shown in Figure 18, or peripheral swelling of the cladding, as shown in Figure 19.

Figure 20 shows local burnout heat flux as a function of average liquid sodium velocity in the test section. Three burnout curves, each apparently increasing with velocity, are evident: the upper curve corresponds to burnout under locally subcooled liquid conditions (320°F), the lowest curve corresponds to locally saturated liquid conditions, and the intermediate curve is for a small degree of local subcooling. However, the velocity dependence largely disappears when the data are corrected for differences in pressure by the data of Peppler and Schlectendahl[3]

7702-5410

Figure 18. Melting of Cladding, Due to Burnout

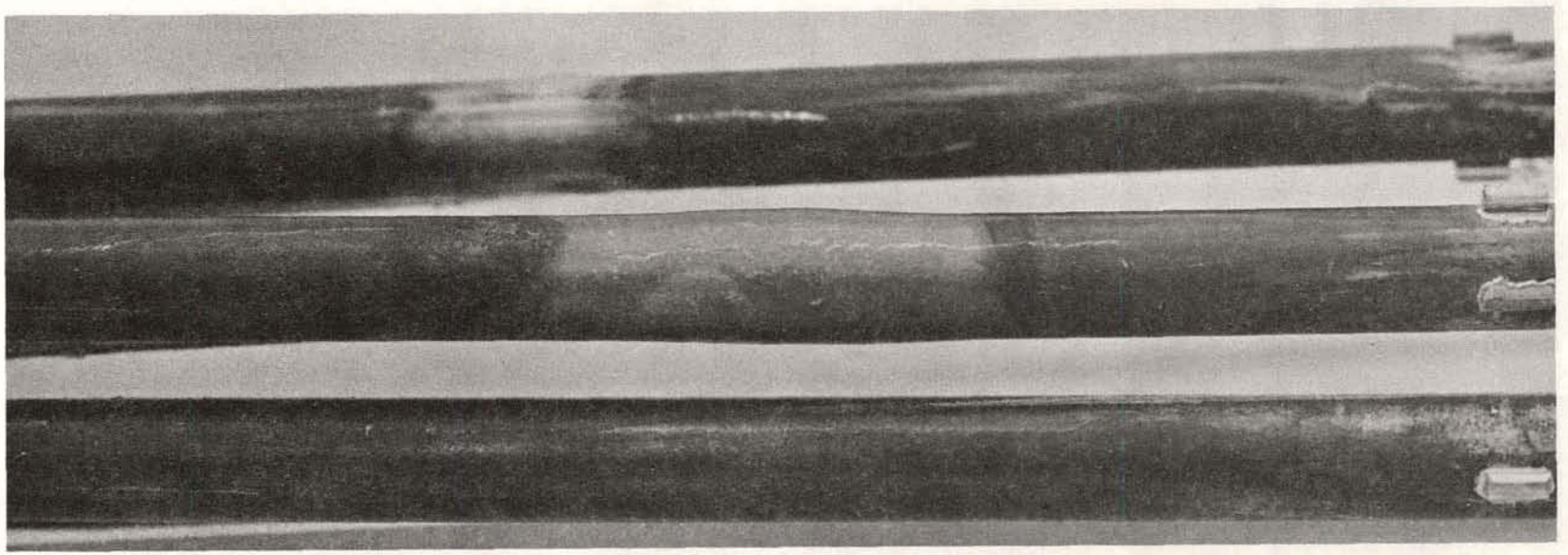

7702-5411

Figure 19. Swelling of Cladding, Due to Burnout

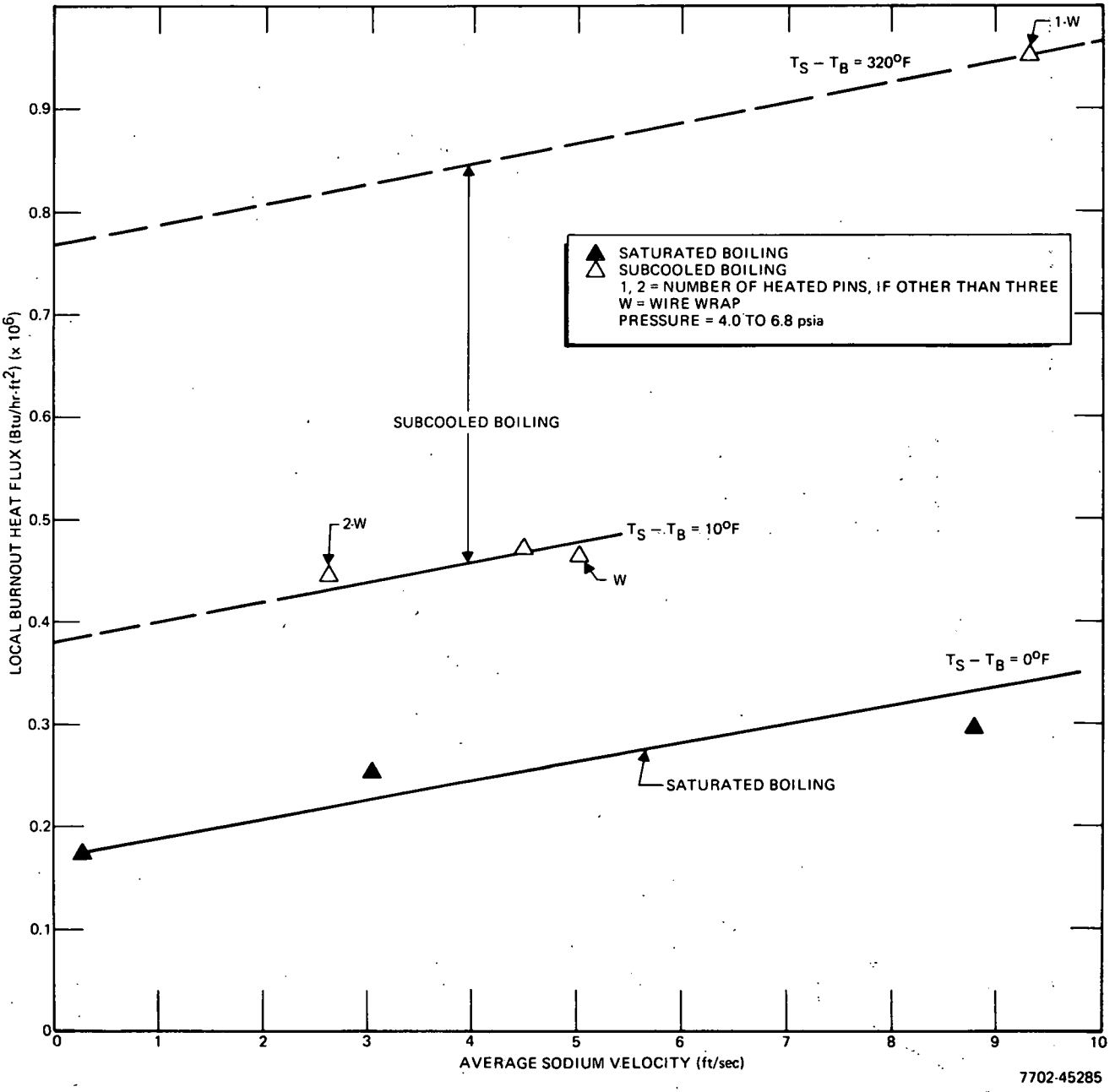

Figure 20. 3-Pin Burnout Data

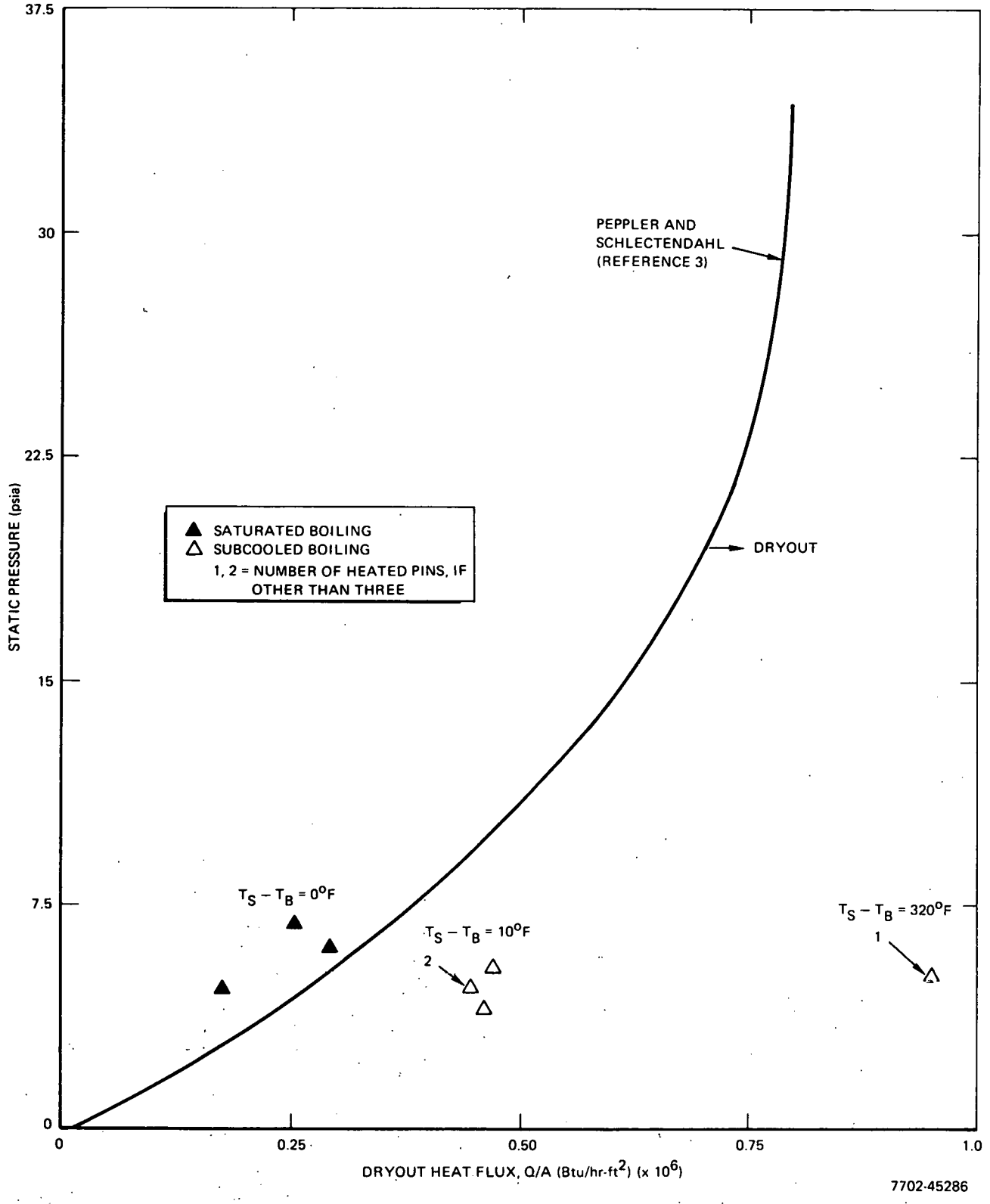

Figure 21. Dryout Heat Flux vs Static Pressure in the Test Section

shown in Figure 21. The increase of burnout heat flux with increasing subcooling shown in Figure 22 is in accord with previous experimental results with water[4] and sodium.[5]

The variation of bulk temperature in the tricuspid area located just above the end of the heated section, and the accelerometer output, are shown in Figure 23, as burnout was approached by successive flow-rate reductions at a heat flux of 450,000 Btu/ft-hr. (Total input power was 32.4 kw.) Initially, the boiling was stable, although the temperature trace shows considerable variation (~100°F). This region appears to correspond to the "stable pulsating boiling" observed by Schleisiek.[6] Twenty seconds before burnout, a small additional flow reduction was made. This lead to a tighter, rising temperature pattern, corresponding to a more uniform and greater vapor generation rate. An identical pattern of behavior is indicated by the accelerometer trace. During this period, the bulk fluid temperature increased from a subcooled state to that approaching saturation. As the bulk temperature of the subcooled fluid increased, a greater fraction of the void generated at the wall continued to survive downstream, until the void fraction was great enough to permit a dryout to occur. A trend, identical to that shown here (increasing temperature), for wall temperature as burnout was approached has been observed for both sodium[6] and water.[7]

For a single annular channel, Peppler and Schlectendahl[3] have determined the region of sodium burnout in terms of pressure level only. The present saturated boiling data fall near the dryout zone described by these authors, while the slightly subcooled data are displaced toward higher burnout heat fluxes. Since, in a multichannel configuration, local conditions which affect burnout (mass velocity, quality, subcooling) can differ greatly from that of the average, or single-channel, conditions, and present favorable comparison with the single-channel results may be fortuitous. As a result, further multichannel burnout data at higher static pressures (i.e., 15 and 30 psia) are required for LMFBR accident analyses.

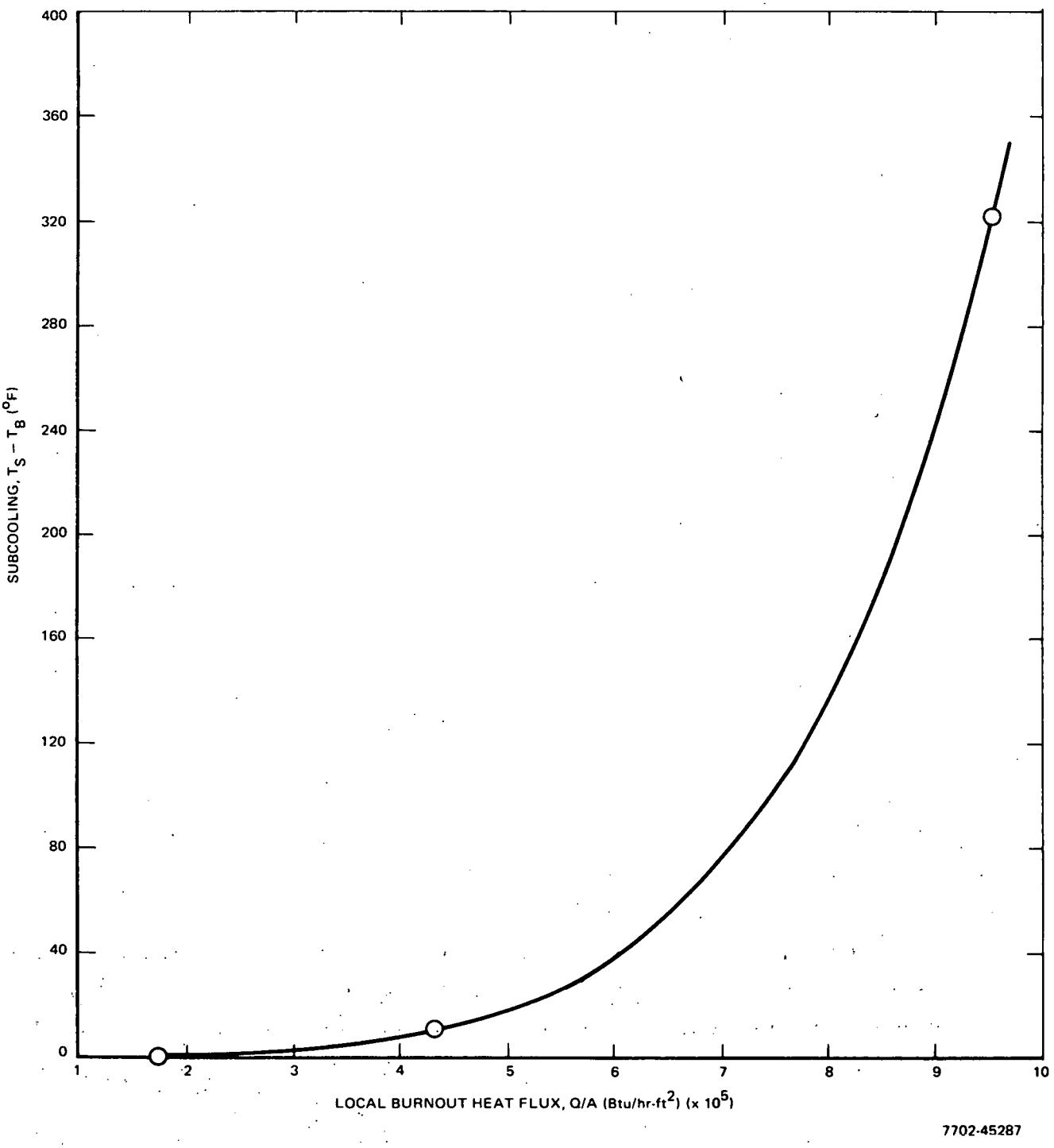

Figure 22. Subcooling vs Local Burnout Heat Flux (Pressure corrected to 5-psia data of Peppler and Schlectendahl, Reference 3)

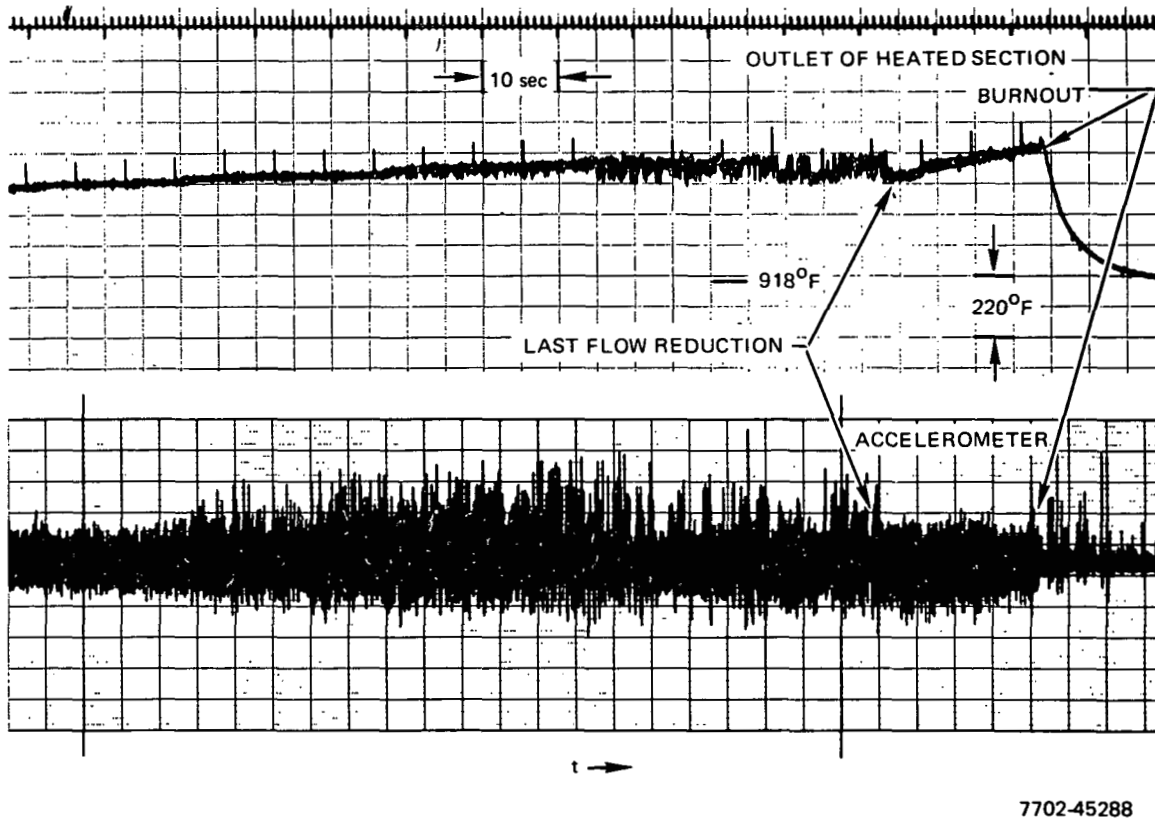

Figure 23. Traces for Burnout at 32.4 -kw Total Power

IV. CONCLUSIONS

Two-phase thermal-hydraulic tests in multichannel LMFBR geometry showed the existence of a loop check curve, in which pressure drop remained essentially constant until boiling was attained in all channels. This verified the predictions of SODIFAZE, a multichannel boiling sodium code. The shape of the multichannel check curve was shown to be very sensitive to differences in channel heat input or dimensions.

Boiling sodium pressure drop behavior in a multichannel test section with equal-length heated and unheated sections showed a pronounced hysteresis effect when decreasing flow is followed by increasing flow.

At ~5 psia and heat fluxes of ~200,000 Btu/hr-ft^2, it was possible to produce multichannel check curves extending well into the two-phase region. However, at heat fluxes >400,000 Btu/hr-ft^2, subcooled boiling, with negligible vapor generation, occurred, and burnout was observed shortly after the two-phase region was entered.

It was shown that, at 5 psia, velocity effects on pressure-corrected burnout heat flux data were small, while the effects of subcooling on burnout heat flux were large.

REFERENCES

1. C. J. Baroczy, "SODIFAZE, A Steady State Multichannel Boiling Sodium Code," AI-AEC-12804 (February 15, 1970)

2. D. Logan, C. J. Baroczy, J. A. Landoni, and H. A. Morewitz, "Studies of Boiling Initiation for Sodium Flowing in a Heated Channel," AI-AEC-12767 (September 30, 1969)

3. W. Peppler and E. G. Schlectendahl, "Experimental and Analytical Investigations of Sodium Boiling Events in Narrow Channels," Liquid Metal Heat Transfer and Fluid Dynamics, ASME Symposium, New York, November 30, 1970

4. L. S. Tong, F. E. Motley, and J. O. Cermak, "Scaling Law of Flow-Boiling Crisis," Vol. VI, Fourth International Heat Transfer Conference, Paris, 1970

5. R. C. Noyes and H. Lurie, "Boiling Sodium Heat Transfer," Vol. V, Third International Heat Transfer Conference, Chicago, Illinois, August 7-12, 1966

6. K. Schleisiek, "Heat Transfer and Boiling During Forced Convection of Sodium in an Induction-Heated Tube," Nuc. Eng. and Design, 14 (1970) p 60

7. M. P. Fiori and A. E. Bergles, "Model of Critical Heat Flux in Subcooled Flow Boiling," Vol. VI, Fourth International Heat Transfer Conference, Paris, 1970

Atomics International
North American Rockwell

P.O. Box 309
Canoga Park, California 91304